

# Bayesian Admission Policies for Cloud Computing Clusters

Ludwig Dierks<sup>1</sup>, Ian Kash<sup>2</sup>, and Sven Seuken<sup>1</sup>

<sup>1</sup> Department of Informatics, University Zurich

<sup>2</sup> Department of Computer Science, University of Illinois at Chicago

dierks@ifi.uzh.ch, iankash@uic.edu, seuken@ifi.uzh.ch

## Abstract

Cloud computing providers must handle customer workloads that wish to scale their use of resources, such as virtual machines, up and down over time. Currently, this is often done using simple threshold policies to reserve large parts of each cluster. This leads to low average utilization of the cluster. In this paper, we propose more sophisticated Bayesian policies for controlling admission to a cluster and demonstrate that they significantly increase cluster utilization. We first introduce a model for the cluster admission problem and fit its parameters on a data trace from Microsoft Azure. We then design Bayesian cluster admission policies that estimate moments of each workload’s distribution of future resource usage. Via simulations we show that, while estimating the first moments of workloads leads to a substantial improvement over the simple threshold policy, also taking the second moments into account yields another improvement in utilization. We then evaluate how much further this can be improved with learned or elicited prior information and how to incentivize users to provide this information.

## 1 Introduction

Cloud computing is a fast expanding market with high competition where small efficiency gains translate to multi billion dollar profits.<sup>1</sup> Nonetheless, most cloud clusters currently run at very low average utilization. Some of this is caused by purely technical limitations, such as the need to reserve capacity for node failures or maintenance, outside factors such as fluctuations in overall demand, or inefficiencies in scheduling procedures, especially if virtual machines (VMs) might change size or do not use all of their requested capacity [Yan *et al.*, 2016]. Another cause is the nature of many modern workloads: highly connected tasks running on different VMs that should be run on one cluster to minimize latency and bandwidth use [Cortez *et al.*, 2017]. In practice, this means that different VMs from one user are bundled together into a *deployment* of interdependent workload. When the workload of a deployment changes, it can request a *scale out* in the form of additional VMs or shut some of its active VMs

<sup>1</sup><https://www.microsoft.com/en-us/Investor/earnings/FY-2018-Q2/press-release-webcast>

down. Scale out requests should almost always be accepted on the same cluster, as denying them would impair the quality of the service, possibly alienating customers. Providers consequently hold large parts of any cluster as idle reserves to guarantee that only a very low percentage of these requests is ever denied.

### 1.1 Cluster Admission Control

Thus, an important decision is which cluster a new deployment is assigned to. We reduce this to the problem of determining, for a particular cluster, whether to admit a deployment for scheduling or if doing so would risk running out of capacity if the deployment scales [Cortez *et al.*, 2017]. While a lot of research has been done on scheduling *inside* the cluster [Schwarzkopf *et al.*, 2013; Verma *et al.*, 2015; Tumanov *et al.*, 2016], the admission decision has not been well studied before. Consequently, cloud providers are still often using simple policies like thresholds on the current utilization of a cluster.<sup>2</sup> These seem reasonable at first glance, as the law of large numbers might suggest that the overall utilization carries most information for large clusters. But as Cortez *et al.* [2017] have shown, a relatively small number of deployments account for most of the utilization. This suggests that the specific deployments in a cluster have a larger impact on the failure probability than is apparent.

### 1.2 Overview of Contributions

In this paper, we present *Bayesian admission policies* that infer and use probabilistic information about a cluster’s population to achieve a significantly higher overall utilization with a reduced risk of running out of capacity. For this, we first present a succinct mathematical formulation of the cluster admission problem as it presents itself to cloud providers.

We then give a statistical model for the typical population of deployments in clusters and for how each deployment changes over time. We base this on an extensive analysis and fitting of a data trace from a real-world cloud computing center (Microsoft Azure internal jobs [Cortez *et al.*, 2017]).

Next, we design more sophisticated cluster admission policies that take advantage of learned information. These policies evaluate the moments of our statistical model, but can also be adapted to different models. The insight that makes

<sup>2</sup>This is common knowledge inside the industry and was additionally confirmed to us in communications with various domain experts. However, to the best of our knowledge, there exists no publicly available written source.

these policies possible is that substantial information can be learned about the future behavior of a deployment by observing its behavior while it is in the system. In simulations, we show that using this learned information to estimate the mean future size of deployments already results in a substantial gain in utilization. Incorporating information about the variance then adds another additional improvement. Finally, we examine how our results can be improved if there is additional information available about a deployment at the time the admission control decision must be made. We give a simple framework which captures a notion of the quality of information available, and through additional simulations quantify how the policies benefit from this additional information. Finally, we present a new *information elicitation approach*, introducing a variance-based pricing rule to elicit labels from users. This rule provides users with the right incentives to (a) label their deployments properly (into high and low variance deployments) and (b) use deployments that help the cluster run more efficiently.

## 2 Preliminaries

### 2.1 The cluster admission problem

We consider a single cluster in a cloud computing center. A cluster consists of  $c$  *cores* that are available to perform work.  $c$  is also called the cluster's *capacity*. These cores are used by *deployments*, i.e. interdependent workloads that use one or more cores. The set of deployments currently on the cluster is denoted by  $X$ , and each deployment  $x \in X$  is assigned a number of cores  $C^x$ . Any core that is assigned to a deployment is called *active*, while the remainder are *inactive*. All inactive cores are assumed to be ready to be assigned and become active at any time.<sup>3</sup>

The exact placement of cores inside the cluster is not taken into account at this level and in consequence we do not model the grouping of cores into VMs. A deployment can request to *scale out*, i.e. increase its number of active cores. Each such request is for one or more additional cores and must be accepted whenever activating the requested number of cores would not make the cluster run over capacity. Following current practice, scale out requests must be granted entirely or not at all. Deployments may also stop using some of their cores over time and these cores then become inactive. A deployment *dies* when its number of active cores becomes zero. It can also die spontaneously, instantly making all of its cores inactive. Intuitively this models a decision by a user to shut down the deployment.<sup>4</sup>

New deployment requests arrive over time and are accepted or rejected according to an admission *policy* based on the current state of the cluster and the arriving deployment. The policy has to make sure that the cluster is not forced to reject a higher percentage of scale out requests than is specified by the internal *service level agreement* (SLA)  $\tau$ . If a scale out

<sup>3</sup>While this is an abstraction, effects that make inactive cores become unavailable, such as hardware failure or capacity reserved for maintenance, are independent of the cluster admission policy. They therefore do not affect the relative efficiency of policies and don't need to be modeled.

<sup>4</sup>We model death as permanent because with no active cores any future request could be assigned to a different cluster.

request cannot be accepted because the cluster is already at capacity, one failure for the purpose of meeting the SLA is logged per requested core. An optimal policy therefore maximizes the *utilization* of the cluster, i.e. the average number of active cores, while making sure the SLA is observed in expectation (i.e., over time).

### 2.2 Data Trace

We fitted the behavior of deployments to the data trace published by Cortez et al. [2017].<sup>5</sup> This dataset consists of one month of data of internal Microsoft Azure jobs. It contains 35,576 deployments, but only 29,757 of these, those that arrived during the observed time period, can be used for fitting without getting skewed towards long lived deployments. The rest were culled from the dataset. The 29,757 deployments activated 4,317,961 cores, out of which 4,211,926 became inactive again during the observed month.

The exact lifetime of the remaining cores (i.e. the length of time between becoming active and then inactive again) is not known; instead we only have a lower bound on it (i.e. our observation is Type I censored: see for example [NIST, 2012]). Thus, for cores where we only have a lower bound on the lifetime we use the cdf in our likelihood function while for cores whose lifetime is known we use the pdf.

### 2.3 Fitting on the deployment level

We assume that the processes for the time between scale out and the time until a core becomes inactive are both memoryless. This is common whenever arrival and departure processes are modeled such as in queuing theory, and has been used in previous models of cloud computing [Abhishek et al., 2012; Dierks and Seuken, 2016]. Consequently, we fit a Poisson distribution to the scale out rate of each deployment, while we fit an exponential distribution to the lifetime of cores for each deployment that had at least one core become inactive during the observed time period. To fit the size of a scale out, we used a Poisson distribution (plus 1 as scale outs must have at least one core).<sup>6</sup>

### 2.4 Fitting on the population level

Once we had distributions for each deployment we turned to fitting prior distributions for the population. We need those to produce a realistic mix of arriving deployment to evaluate the impact of any policy through simulations. As the data was skewed, positive, and not really heavy tailed, a Gamma Distribution is a natural and very general candidate (containing the Chi-squared, Erlang and Exponential distributions as special cases). We compared it to a few other potential distributions (Weibull, Lognormal, Lomax) and it indeed resulted in the best fit by a large margin. The resulting model and parameters from our fits are shown in Table 1. While the scale out

<sup>5</sup>In contrast to [Cortez et al., 2017] we did not consolidate all deployments a single user runs on a certain day into one. This is because cores that get requested as a new deployment do not need to be accepted on the same cluster.

<sup>6</sup>As the Poisson distribution is single-parameter and its variance cannot be set independent of the average size, this is not a good fit for users with large but consistent scale out sizes. However, its simplicity avoids overfitting on the often low number of samples per deployment and it results in a good fit on the population level.

Table 1: Fitted processes

Deployment processes	scale out process	scale out size distribution	core lifetime distribution	deployment lifetime distribution
Distribution	Poisson( $\Lambda M$ )	Poisson( $\Sigma$ )	Exponential( $M$ )	Exponential( $\Delta M$ )
Deployment parameters	normalized scale out rate $\Lambda$	average scale out size $\Sigma$	core lifetime rate $M$	deployment lifetime rate per core lifetime $\Delta$
Prior	Gamma(0.3494, 0.1543)	Gamma(0.2705, 0.0571)	Gamma(0.3190, 0.5932)	0.0337

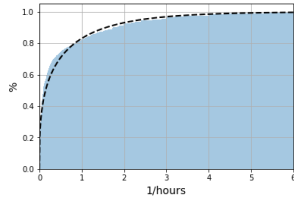


Figure 1: Distribution of core lifetime rate parameters

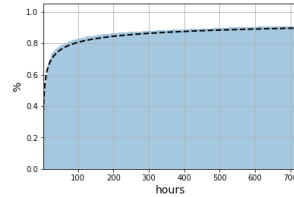


Figure 2: Distribution of core lifetimes

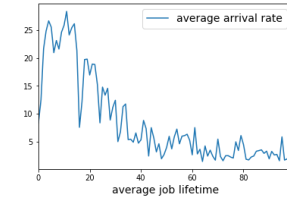


Figure 3: Scale out rate as a function of average core lifetime

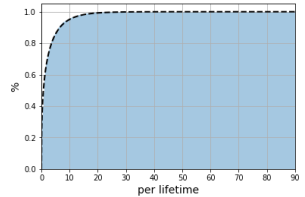


Figure 4: Distribution of scale out rate parameters

size is fit directly to the samples, scale out rate and core lifetime are highly correlated. The longer a deployment’s cores live, the lower the rate at which new cores arrive, as can be seen in Figure 3. This is interesting, as it means that deployments with long lived cores do not necessarily have more active cores. To account for it, we normalized all scale out rates by the respective core lifetimes.

To visualize the fitted distributions, Figure 1 shows the cdf of the Gamma Distribution for the lifetime parameter, overlaid over the normalized cumulative histogram of the fitted rates of the sample deployments. Figure 2 shows the cdf over the lifetime of a core from a random deployment in our model over the normalized cumulative histogram of one core, drawn randomly from each deployment that started in the first seven days.<sup>7</sup> It only shows cores that are started early, as the realized lifetime of later cores is evermore skewed by the time left until the end of the observed month. Visually, our prior produces an excellent fit to the data.

Figure 4 shows the cdf for the normalized scale out rates over the relevant cumulative histogram. The actual scale out rate of a sampled deployment is now simply the normalized scale out rate multiplied by the average core lifetime. Figure 5 shows the fitted cdf for scale out size parameters over its cumulative histogram. Figure 6 shows the probability mass function of drawing a random scale out from a randomly drawn deployment in our model over the histogram of the size of one scale out event drawn randomly from each deployment in the data set. This shows that the mix of scale out sizes in the simulated population based on our priors is roughly equal to the data trace.<sup>8</sup>

<sup>7</sup>Note that this cdf takes the form of a Lomax distribution as the convolution of a Gamma and an Exponential distribution.

<sup>8</sup>Note that Azure only offers VMs whose core counts are a power of two.

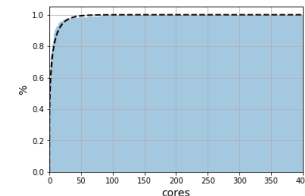


Figure 5: Distribution of scale out size parameters

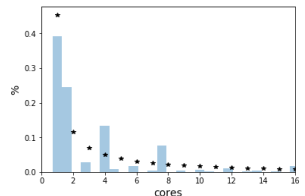


Figure 6: Distribution of scale out sizes

**Deployment Shutdown.** While most deployments in the dataset die because they have zero active cores, 5,980 of the 22,241 deployments that both arrive and die during the observed period seem to get actively shut down. By this we mean that they had at least 3 VMs that all shut down simultaneously. This would be highly unlikely if deployments only die when cores or VMs become inactive independently. To capture such behavior we fit an exponential distribution over the number of expected core lifetime deployments lived. The maximal lifetime of deployments that did not get shut down was assumed to be censored to their realized lifetime.

### 3 Admission Control Policies

In this section, we present the cluster admission policy currently used in practice, as well as our new, more sophisticated Bayesian policies. Any cluster utilizes a policy that decides whether an arriving deployment is accepted into the cluster or not. Current policies simply take the utilization of a cluster as input. If a cluster had further (more precise) information about the current population of deployments and their future behavior, it could accept more deployments whenever the current set of deployments allows it. Even if no information about specific arriving deployments is available upfront, a simple population-wide prior can usually be constructed. This allows the parameters of running deployment to be inferred at runtime. While a deployment is running, samples

from their distributions can be collected. In this paper, we assume that these samples are used for simple Bayesian updating of the prior. This means the cluster gains a good level of information on longer running deployments.

### 3.1 Zeroth Moment Policy (Baseline)

The baseline for admission control policies that is widely used in practice is a myopic policy that simply compares the current number of active cores to a threshold. This policy does not require any information about the set of deployments besides the total number of active cores. We also call it *Zeroth Moment Policy*, because it takes no information about the future into account. The limited amount of information it uses means that it has to be very conservative in how many deployments to accept, since it does not know how often or fast they will scale out.

**Definition 1** (Zeroth Moment policy). *With a zeroth moment policy with threshold  $t$ , a newly arriving deployment is accepted if after accepting the deployment there would be less than  $t$  cores active in the cluster.*

### 3.2 First Moment Policy

Our first policy that takes learned information about the current set of deployments into account uses the first moments of the deployment processes, i.e. the mean, to predict the expected utilization in future time steps, under the assumption that the arriving deployment but no further deployments are accepted. If the expected utilization lies above some chosen threshold, the arriving deployment is rejected, otherwise it is accepted. To keep the problem tractable, we discretize time. In particular, we calculate the expected utilization at a fixed set of points in the future, which we call *timesteps*. The current time is normalized to timestep 0.

**Definition 2.** *We describe the evolution of a deployment  $x$  using the following random variables. All have an implicit superscript  $x$ , which we omit when clear from context.*

- $C$  is the variable denoting the number of active cores at timestep 0.
- $Y_i$  is the random variable denoting the number of scale outs that occur between timestep  $i - 1$  and timestep  $i$ , assuming the deployment has not died.
- $S_{i,l}$  is the size the  $l$ 'th scale out request would have, assuming at least  $l$  scale out requests occur between timestep  $i - 1$  and timestep  $i$ .
- $Z_{n,i,k}$  is the binary random variable denoting whether the  $k$ 'th core activated between timesteps  $i - 1$  and  $i$  would still be active in timestep  $n$ , assuming at least  $k$  cores were activated and the deployment has not died. If  $i = 0$ , this refers to the set of cores already active at timestep 0.
- $D_i$  is the random variable which is 1 if  $x$  would not have died due to a lack of active cores before timestep  $i$ . It can be defined recursively as

$$D_i = D_{i-1}(1 - \prod_{k=1}^C (1 - Z_{i,0,k})) \quad (1)$$

$$\prod_{j=1}^{i-1} \prod_{k=1}^{Y_j} S_{j,k} (1 - Z_{i,j,k})) \quad (2)$$

$$D_1 = 1 - \prod_{k=1}^C Z_{1,0,k} \quad (3)$$

- $B_n$  is the random variable denoting the number of cores that were active at timestep 0 and are still active in timestep  $n$ , which can be calculated as

$$B_n = \sum_{k=1}^C Z_{n,0,k}. \quad (4)$$

- $Q_n$  is the random variable denoting the number of cores activated between timestep 0 and timestep  $n - 1$  that are still active assuming no service termination, i.e.

$$Q_n = \sum_{i=1}^{n-1} \sum_{k=1}^{Y_i} S_{i,k} Z_{n,i,k}. \quad (5)$$

- $\Omega_i$  is the random variable which is 1 if the maximum lifetime of the deployment is at least  $i$  and 0 otherwise.
- Finally,  $L_n$  is the random variable denoting the number of active cores in timestep  $n$  which can be calculated as

$$L_n = \Omega_n D_n (Q_n + B_n). \quad (6)$$

This allows us to define a policy that does not simply bound the number of active cores in the cluster (as the Zeroth Moment Policy does), but instead bound's how many cores are expected to be active in the future.

**Definition 3** (First Moment Policy). *With a first moment policy with threshold  $t$ , a newly arriving deployment is accepted whenever after accepting the deployment the expected number of active cores would be less than  $t$  in all future timesteps, i.e.*

$$\sum_{x \in X} E[L_n^x] \leq t \quad \forall n \quad (7)$$

Note that, unless the exact parameters of a deployment are known, all  $Y_i$ , all  $S_{i,l}$  and all  $Z_{n,i,k}$  are highly correlated. While the expectations of  $Q_n$  and  $B_n$  can easily be expressed in the expectations of their component random variables, solving  $D_n$  is very hard for most distributions. In practice, it therefore is usually preferable to only approximate  $D_n$ . Similarly, ignoring the correlation between the  $Q_n$ ,  $D_n$  and  $B_n$  greatly simplifies policy evaluation and does not overly impact the prediction quality. Thus, our policy uses the following mix of exact and approximate moments.

**Proposition 1.** *It holds:*

$$E[L_n] \approx E[\Omega_n] E[D_n] (E[Q_n] + E[B_n]) \quad (8)$$

$$E[Q_n] = \sum_{i=1}^{n-1} E[E[Y_i | \lambda, \mu] E[S_{i,1} | \sigma] E[Z_{n,i,1} | \mu]] \quad (9)$$

$$E[D_i] \approx E[D_{i-1}] (1 - (1 - E[Z_{i,0,1}])^{(C)}) \quad (10)$$

$$\prod_{j=1}^{i-1} (1 - E[Z_{j,1}])^{E[Y_j] E[S_{j,1}]} \quad (11)$$

$$E[D_1] = (1 - (1 - E[Z_{1,0,1}])^{(C)}) \quad (12)$$

$$E[B_n] = C E[Z_{n,i,k}] \quad (13)$$

The proof can be found in the supplementary material. There we also present the expressions instantiated for the distributions fitted on the data trace, which we will later use in our simulation experiments.

As part of calculating the specific expressions, which are non-trivial, we make an additional assumption that no core activated between timesteps  $i - 1$  and  $i$  becomes inactive before timestep  $i$ . This is also the reason why  $Q_n$  only considers cores activated up to timestep  $n - 1$ .

### 3.3 Second Moment Policy

First moment policies still fail to take into account much of the structure of deployments. In a sense they always have to take the worst possible population mix into account and run the risk of accepting deployments with low expected size but high variance when close to the threshold. One way around this is to also take the second moment, i.e. the variance of  $L_n$ , into account. Measuring the threshold in active (current or predicted) cores does not make sense here. Instead we can use Cantelli's inequality, a single-tailed generalization of Chebyshev's inequality, to bound the probability of going above capacity given the current population.

**Proposition 2** (Cantelli's Inequality). *For any real valued random variable  $L$  and any  $\epsilon \geq 0$  it holds*

$$\Pr(L - E[L] \geq \epsilon) \leq \frac{\text{Var}[L]}{\text{Var}[L] + \epsilon^2} \quad (14)$$

If we now set  $\epsilon = (c - \sum_{x \in X} E[L_n^x])$ , we can bound the probability of running over capacity. While the bound given by the inequality is not tight enough to simply set it to  $\tau$ , it can be used to bound the first two moments in a systematic way.

**Definition 4** (Second Moment Policy (Cantelli Policy)). *With a Cantelli policy with threshold  $\rho$ , a newly arriving deployment is accepted if the estimated probability of running over capacity in all further timesteps is less than  $p$ , i.e.*

$$\frac{\sum_{x \in X} \text{Var}[L_n^x]}{\sum_{x \in X} \text{Var}[L_n^x] + (c - \sum_{x \in X} E[L_n^x])^2} \leq \rho \quad \forall n \quad (15)$$

The variance is more complex to calculate than the expectation. Our general approximation result, again ignoring some of the covariance, is given by the next proposition.

**Proposition 3.** *It holds:*

$$V[L_n] = E[\Omega_n]V[D_n Q_n] \quad (16)$$

$$+ E[\Omega_n](1 - E[\Omega_n])E[D_n Q_n]^2 \quad (17)$$

$$V[D_n Q_n] \approx E[D_n]V[Q_n] \quad (18)$$

$$+ E[Q_n]^2 E[D_n](1 - E[D_n]) \quad (19)$$

$$V[Q_n] = E[V[Q_n|\lambda, \sigma, \mu]] \quad (20)$$

$$+ V[E[Q_n|\lambda, \sigma, \mu]] \quad (21)$$

$$V[Q_n|\lambda, \sigma, \mu] = \sum_{i=1}^{n-1} ((V[Y_i|\lambda, \mu]E[S_{i,l}|\sigma]^2 \quad (22)$$

$$+ E[Y_i|\lambda, \mu]V[S_{i,l}|\mu])E[Z_{n,i,1}|\mu]^2 \quad (23)$$

$$+ E[Y_i|\lambda, \mu]E[S_{i,l}|\sigma]V[Z_{n,i,1}|\mu]) \quad (24)$$

$$V[D_n] \approx E[D_n](1 - E[D_n]) \quad (25)$$

$$V[B_n] \approx CV[Z_{n,i,k}] \quad (26)$$

The proof, as well as the specific variance expressions for our fitted processes are omitted for space constraints and can again be found in the supplementary material.

#### Computational overhead.

The computational overhead of the second moment policy depends on the number of future timesteps it evaluates. Fortunately, each single rule application is fast. Updating the estimate for the second moment policy for a single deployment,

i.e. solving (15), is in  $O(n^2)$  where  $n$  is the number of evaluated timesteps. Whenever a new deployment arrives, the estimate is updated for every active deployment. This leads to a worst case runtime of  $O(|X|n^2)$  where  $|X| \leq c$  is the number of active deployments. For multiple clusters this is fully parallelizable at the cluster level because each cluster has its own policy evaluation. Updating the prior of a deployment during runtime has negligible complexity ( $O(1)$ ). A cloud computing center consisting of clusters of capacity  $c$  with an arrival rate of  $L$  new deployment requests per hour therefore has a computation overhead of at most  $O(Lcn^2)$  each hour, parallelizable into jobs of size  $O(n^2)$ . This number can further be significantly reduced in practice by employing smart caching and by updating the estimates only whenever parameters change significantly.<sup>9</sup> This means that even relatively large look-ahead horizons  $n$  can easily be implemented in practice.

## 4 Empirical Evaluation

In this section, we evaluate the performance of our admission policies using the fitted model we have presented in Section 2.4.

<sup>10</sup> We simulated clusters with capacity  $c = 10,000$  for a 1-year period with all three policies. We determined the optimal threshold for each policy via binary search, subject to meeting an SLA of 0.01%. An average of 6 new deployments per hour arrived according to a Poisson process. The parameters of each arriving deployment were drawn from the fitted distributions presented in Table 1. To simulate a full year with a reasonable number of core-hours, the first and second moment policies both only looked ahead 2 hours, discretized in 12 timesteps. This means that the policies assumed that new scale out requests only arrive every 10 minutes. Note that such a short look ahead would not be required in practice, as calculating the same precision of a single deployment for one month only takes 5 core seconds and only needs to be done whenever a deployment's learned information changes notably. Each simulation was repeated 20 times. Each simulation was run on a single core of an Intel E5-2680 v2 2.80GHz processor. The combined runtime of all simulations was about 1,000 core hours.

The results are summarized in Table 2. The zeroth moment policy obtains its best result with a threshold of  $t = 8564$ , i.e. new deployments are accepted whenever less than 8563 would be active in case of acceptance. This results in an average utilization of 87.45 over the lifetime of the cluster. Note that this is higher than would be obtained in reality, as we do not model buffers for hardware failures, etc. The first moment policy with threshold  $t = 8794$  increases utilization by

<sup>9</sup>If further ML is (optionally) employed to obtain an individual prior for arriving deployments (as discussed in Section 5), that computation time would need to be added and depends on the algorithm in question.

<sup>10</sup>Note that our dataset only covers one month. This is too short to fully evaluate cluster admission policies because many effects only show up after months of usage. Instead, we use our behavioral model, fitted to the data we do have, to simulate longer time periods (1 year, in our simulations). We defer evaluations against real deployments to future work once more data is available.

Table 2: Simulation results

Policy	Threshold	Utilization	Standard Error
Zer0th Moment	$t = 8564$	87.45	0.0619
First Moment	$t = 8794$	89.38	0.0685
Second Moment	$\rho = 0.0004$	91.17	0.1302

1.93 to 89.38, a relative increase by 2.21%. This means that the same number of deployments can be served by roughly 2% less hardware. While this might not seem much at a first glance, reducing hardware requirements by even a single percent saves hundredth of millions of dollars over the hardware lifetime, which go directly into gross profits instead. This is an invaluable competitive edge. The second moment policy with threshold  $\rho = 0.00039$  achieves a utilization of 91.1, which constitutes a relative increase of 4.25% over the zeroth moment policy and of 2% over the first moment policy. This shows that taking the second moment into account greatly improves the usefulness of learning parameters during runtime.

## 5 Learned or Elicited Prior Information

So far, the policies did not have any information about deployments that arrive besides their initial number of cores and therefore have to make the acceptance decision primarily based on the current state of the cluster. Intuitively, policies could more precisely control whether accepting a deployment would risk violating the SLA if they had more information about its future behavior. One way to obtain such information would be to use machine learning (ML) based on features of the arriving deployment and past deployment patterns of the submitting user [Cortez *et al.*, 2017]. While evaluating particular ML algorithms is beyond the scope of this paper, we evaluate the effect different levels of available information have. To do this we need to parametrize the level of knowledge. For this we assume that we simply have some number of samples from the true distribution.<sup>11</sup>

### 5.1 Empirical Evaluation of Prior Information

We simulated the first and second moment policies with varying numbers of prior observations. The short look-ahead of 2 hours now poses a problem because long lived, slow scaling deployments are estimated to be very small in the look-ahead period, yet will in fact grow large over time.<sup>12</sup> Therefore we implemented the following heuristic: any arriving deployment is assumed to have  $\Gamma \Sigma M^2$  active cores, the expected average size it would be if being allowed to stay in the cluster forever without dying.<sup>13</sup> If accepted, a deploy-

<sup>11</sup> Note that, as we have used conjugate prior distributions in our model, this approach matches the standard interpretation of parameters of the posterior distribution in terms of pseudo-observations.

<sup>12</sup>This does not happen in the prior free version, as the learning during runtime only slowly reduces the scaling speed of large, long-lived deployments.

<sup>13</sup>This equals its steady state size according to Little’s Law from queuing theory. While this heuristic could be used with the zeroth

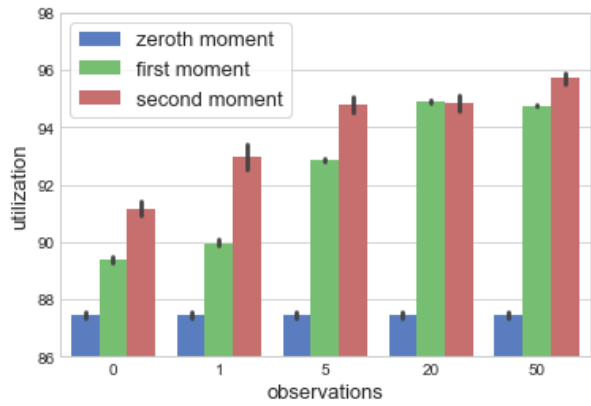


Figure 7: Performance of different policies depending on prior information (error bars indicate standard errors)

ment still only arrives with the drawn arrival size equal to one scale out. We run simulations with 5 different levels of information (0,1,5,20,50 observations), with the same setup as in Section 4 and 20 runs each. These simulations took 3300 core-hours. The results are shown in Figure 7. We see that having prior knowledge equivalent to a single sample would improve utilization significantly. Increases the amount of information does then further reduce the amount of cores that stand idle. With the equivalent of 50 observations, utilization is increased by up to 9% over the baseline. This means the provider requires about 9% less hardware to run the same number of deployments, greatly reducing costs and increasing profits. Further, at any level of information the second moment policy tends to outperform the first.

### 5.2 Elicited Prior

While using machine learning to predict the parameters of deployments is powerful, users typically do not submit deployments with arbitrary parameters. Instead, they may have a small number of different *types* of deployments. While sophisticated machine learning may be able to learn this, it may be better to directly elicit some information from the users. However, asking for estimates of parameters for a given deployment is problematic, as it either shifts risk to the consumer or enables manipulation. This leads to the idea of getting users to categorize their deployments into different types, with each type consisting of roughly similar deployments. Learning priors for each individual type could then result in more precise priors and higher efficiency.

Typically, users are charged a fixed payment per hour for each core their deployment uses. To this, we now add a small additional charge based on our estimate of the variance of the deployment and allow users to label the type of their deployments, resulting in an hourly payment rule of the form

$$\pi(X) = (\kappa + \text{Var}(X))C^X, \quad (27)$$

where  $\kappa$  is a constant and  $\text{Var}(X)$  is an estimate of the variance of the deployment. A payment rule of this form incentivizes users to assign similar labels to similar deployments to minimize the estimated variance.

moment policy as well, we found that this decreases utilization.

To see this, consider a user who has two types of deployment,  $x$  and  $y$ , with true variances  $Var(x)$  and  $Var(y)$ . He could now simply submit the deployments under a single label. For the provider, this means that each submitted deployment is of either type with a certain probability, which increases the variance of his prediction. But if the user would label his deployments instead, the provider would know for each arriving deployment which type it is drawn from, reducing variation and therefore the need to reserve capacity. The following proposition, which is immediate from the law of total variance, then shows that, at least in the long run, labeling his deployments also reduces a user’s payments.

**Proposition 4.** *Let  $z$  be the mixture that results from submitting one of two types of deployments  $x, y$  chosen by a Bernoulli random variable  $\alpha \sim Bernoulli(p_\alpha)$ , i.e. such that  $z$  is of type  $x$  with probability  $p_\alpha$  and of type  $y$  with probability  $1 - p_\alpha$ . Then it holds*

$$p_\alpha Var(x) + (1 - p_\alpha)Var(y) \leq Var(z) \quad (28)$$

*Proof.* Since  $z$  trivially has finite variance, the law of total variance states:

$$Var(z) = E[Var(z|\alpha)] + Var(E[z|\alpha]) \quad (29)$$

$$\geq E[Var(z|\alpha)] \quad (30)$$

$$= p_\alpha Var(x) + (1 - p_\alpha)Var(y) \quad (31)$$

□

Proposition 4 shows that the user would be better off, on average, by splitting the mixture and submitting the deployments under separate labels. Note that this abstracts away issues of learning and non-stationary strategic behavior; but for reasonable learning procedures we expect a consistent labeling to lead to lower variance than a mixture while learning. Further, this approach not only gives the user correct incentives to reveal the desired information, but actually incentivizes him to improve the performance of the system. In particular, another way he can lower his payment under this scheme (outside the scope of our model) is to design his deployments in such a way that they have lower variance in their resource use. Since more predictable deployments would allow the policy to maintain a smaller buffer, this provides an additional benefit to the efficiency of the system.

How much any given user could ultimately save by labeling his deployments mostly depends how different his deployment types are and on how high the provider sets the charge for variance. A user whose deployments are very uniform will not save much, while a user with some deployments which never scale and some that scale a lot can potentially save quite a bit. Note that how much the provider should charge is not immediately clear. While he would want to set a high price to put a strong incentive on users, he also has to keep his competition from other providers in mind. At what point the loss of market share outweighs the gain in efficiency is an intriguing problem we leave for future work.

## 6 Related Work

While studying which deployments to admit to a cluster, we have abstracted away the question of exactly which resources they should use. A literature on *cluster scheduling*

addresses this [Schwarzkopf *et al.*, 2013; Verma *et al.*, 2015; Tumanov *et al.*, 2016]. In addition, there is work that addresses a different notion of admission control to a cluster, namely how to manage queues for workloads which will ultimately be deployed to that cluster [Delimitrou *et al.*, 2013].

One line of work for cluster scheduling has looked at how multidimensional resources can be fairly divided among deployments. Dominant Resource Fairness [Ghodsi *et al.*, 2011] is an approach that has proved useful in practice [Hindman *et al.*, 2011] and has inspired follow-up work more broadly in the literature on fair division [Parkes *et al.*, 2012; Dolev *et al.*, 2012; Gutman and Nisan, 2012; Kash *et al.*, 2014]

We have examined the value of learning from prior deployments. Other work has explored similar opportunities in the context of resource planning and scheduling in

analytics clusters [Jyothi *et al.*, 2016; Rajan *et al.*, 2016]

There is a large literature on market design challenges in the context of the cloud [Kash and Key, 2016]. Existing work has studied both queueing models where decisions are made online with no consideration of the future [Abhishek *et al.*, 2012; Dierks and Seuken, 2016] and reservation models which assume very strong information about the future [Azar *et al.*, 2015; Babaioff *et al.*, 2017]. Our work sits in an interesting intermediate position where users may have rough information about what type of deployment each is.

## 7 Conclusion

We have studied the problem of cluster admission control for cloud computing. In practice, simple threshold policies are used for this problem. Our simulations, with parameters fit to traces from Microsoft Azure, show the potential gains based on policies which estimate the first and second moments of future cluster occupancy. Utilization could be increased by up to 4.25% just from learning about deployments while they are active in the cluster, reducing hardware costs by around 4%. This can potentially be increased even further if better prior information about arriving deployments is available, for example through learning or elicitation techniques. While each gain is relatively small in percentage terms, they are economically significant. At cloud scale, these savings translate to hundreds of millions of dollars over the course of a hardware lifetime and any dollar saved directly translates to a gross profit increase for the cluster provider.

## References

- [Abhishek *et al.*, 2012] Vineet Abhishek, Ian A. Kash, and Peter Key. Fixed and market pricing for cloud services. In *7th Workshop on the Economics of Networks, Systems, and Computation (NetEcon)*, pages 157–162, 2012.
- [Azar *et al.*, 2015] Yossi Azar, Inna Kalp-Shaltiel, Brendan Lucier, Ishai Menache, Joseph Naor, and Jonathan Yaniv. Truthful online scheduling with commitments. In *EC15*, 2015.
- [Babaioff *et al.*, 2017] Moshe Babaioff, Yishay Mansour, Noam Nisan, Gali Noti, Carlo Curino, Nar Ganapathy, Ishai Menache, Omer Reingold, Moshe Tennenholtz, and Erez Timnat. Era: a framework for economic resource

allocation for the cloud. In *Proceedings of the 26th International Conference on World Wide Web Companion*, pages 635–642. International World Wide Web Conferences Steering Committee, 2017.

[Cortez *et al.*, 2017] Eli Cortez, Anand Bonde, Alexandre Muzio, Mark Russinovich, Marcus Fontoura, and Ricardo Bianchini. Resource central: Understanding and predicting workloads for improved resource management in large cloud platforms. In *Proceedings of the 26th Symposium on Operating Systems Principles*, SOSP ’17, pages 153–167, New York, NY, USA, 2017. ACM.

[Delimitrou *et al.*, 2013] Christina Delimitrou, Nick Bambos, and Christos Kozyrakis. Qos-aware admission control in heterogeneous datacenters. In *ICAC*, pages 291–296, 2013.

[Dierks and Seuken, 2016] Ludwig Dierks and Sven Seuken. Cloud pricing: the spot market strikes back. In *The Workshop on Economics of Cloud Computing*, 2016.

[Dolev *et al.*, 2012] Danny Dolev, Dror G Feitelson, Joseph Y Halpern, Raz Kupferman, and Nathan Linial. No justified complaints: On fair sharing of multiple resources. In *proceedings of the 3rd Innovations in Theoretical Computer Science Conference*, pages 68–75. ACM, 2012.

[Ghodsi *et al.*, 2011] Ali Ghodsi, Matei Zaharia, Benjamin Hindman, Andy Konwinski, Scott Shenker, and Ion Stoica. Dominant resource fairness: Fair allocation of multiple resource types. In *USENIX Symposium on Networked Systems Design and Implementation*, March 2011.

[Gutman and Nisan, 2012] Avital Gutman and Noam Nisan. Fair allocation without trade. In *Proceedings of the 11th International Conference on Autonomous Agents and Multiagent Systems-Volume 2*, pages 719–728. International Foundation for Autonomous Agents and Multiagent Systems, 2012.

[Hindman *et al.*, 2011] Benjamin Hindman, Andy Konwinski, Matei Zaharia, Ali Ghodsi, Anthony D Joseph, Randy H Katz, Scott Shenker, and Ion Stoica. Mesos: A platform for fine-grained resource sharing in the data center. In *NSDI*, volume 11, pages 22–22, 2011.

[Jyothi *et al.*, 2016] Sangeetha Abdu Jyothi, Carlo Curino, Ishai Menache, Shravan Matthur Narayananurthy, Alexey Tumanov, Jonathan Yaniv, Ruslan Mavlyutov, Inigo Goiri, Subru Krishnan, Janardhan Kulkarni, et al. Morpheus: Towards automated slos for enterprise clusters. In *OSDI*, pages 117–134, 2016.

[Kash and Key, 2016] Ian A. Kash and Peter B. Key. Pricing the cloud. *IEEE Internet Computing*, 2016. In Press.

[Kash *et al.*, 2014] Ian A. Kash, Ariel D. Procaccia, and Nisarg Shah. No agent left behind: Dynamic fair division of multiple resources. *Journal of Artificial Intelligence Research*, 51:579–603, 2014.

[NIST, 2012] NIST. Nist/sematech e-handbook of statistical methods. <http://www.itl.nist.gov/div898/handbook/apr/section4/apr412.htm>, 2012.

[Parkes *et al.*, 2012] D. C. Parkes, A. D. Procaccia, and N. Shah. Beyond dominant resource fairness: Extensions, limitations, and indivisibilities. In *ACM Conference on Electronic Commerce (EC)*, June 2012.

[Rajan *et al.*, 2016] Kaushik Rajan, Dharmesh Kakadia, Carlo Curino, and Subru Krishnan. Perforator: eloquent performance models for resource optimization. In *Proceedings of the Seventh ACM Symposium on Cloud Computing*, pages 415–427. ACM, 2016.

[Schwarzkopf *et al.*, 2013] Malte Schwarzkopf, Andy Konwinski, Michael Abd-El-Malek, and John Wilkes. Omega: flexible, scalable schedulers for large compute clusters. In *Proceedings of the 8th ACM European Conference on Computer Systems*, pages 351–364. ACM, 2013.

[Tumanov *et al.*, 2016] Alexey Tumanov, Timothy Zhu, Jun Woo Park, Michael A Kozuch, Mor Harchol-Balter, and Gregory R Ganger. Tetrished: global rescheduling with adaptive plan-ahead in dynamic heterogeneous clusters. In *Proceedings of the Eleventh European Conference on Computer Systems*, page 35. ACM, 2016.

[Verma *et al.*, 2015] Abhishek Verma, Luis Pedrosa, Madhukar Korupolu, David Oppenheimer, Eric Tune, and John Wilkes. Large-scale cluster management at google with borg. In *Proceedings of the Tenth European Conference on Computer Systems*, page 18. ACM, 2015.

[Yan *et al.*, 2016] Ying Yan, Yanjie Gao, Yang Chen, Zhongxin Guo, Bole Chen, and Thomas Moscibroda. Tr-spark: Transient computing for big data analytics. In *SoCC*, 2016.

## Appendix

**Proposition 5.** *It holds:*

$$E[L_n] \approx E[\Omega_n]E[D_n](E[Q_n] + E[B_n]) \quad (32)$$

$$E[Q_n] = \sum_{i=1}^{n-1} E[E[Y_i|\lambda, \mu]E[S_{1,1}|\sigma]E[Z_{n,i,1}|\mu]] \quad (33)$$

$$E[D_i] \approx E[D_{i-1}](1 - (1 - E[Z_{i,0,1}])^{(C)}) \quad (34)$$

$$\Pi_{j=1}^{i-1} (1 - E[Z_{i,j,1}])^{E[Y_1]E[S_{1,1}]} \quad (35)$$

$$E[D_1] = (1 - (1 - E[Z_{1,0,1}])^{(C)}) \quad (36)$$

$$E[B_n] = CE[Z_{n,i,k}] \quad (37)$$

*Proof.* • If  $E[\Omega_n], E[D_n], E[Q_n]$  and  $E[B_n]$  would be uncorrelated, it would hold for the expectation of  $L_n$ :

$$E[L_n] = E[\Omega_n]E[D_n](E[Q_n] + E[B_n]) \quad (38)$$

$$(39)$$

$$(40)$$

As the correlation is limited, especially with more information,

$$E[L_n] \approx E[\Omega_n]E[D_n](E[Q_n] + E[B_n]) \quad (41)$$

$$(42)$$

$$(43)$$

is a reasonable approximation in practice.

•  $Q_n$ : For the expectation it holds:

$$E[Q_n] = E\left[\sum_{i=1}^{n-1} \sum_{k=1}^{\sum_{l=0}^{Y_i} S_{i,l}} Z_{n,i,k}\right] \quad (44)$$

$$= \sum_{i=1}^{n-1} E\left[\sum_{k=1}^{\sum_{l=0}^{Y_i} S_{i,l}} Z_{n,i,k}\right] \quad (45)$$

$$= \sum_{i=1}^{n-1} E\left[E\left[\sum_{k=1}^{\sum_{l=0}^{Y_i} S_{i,l}} Z_{n,i,k} | \lambda, \sigma, \mu\right]\right] \quad (46)$$

$$E\left[\sum_{k=1}^{\sum_{l=0}^{Y_i} S_{i,l}} Z_{n,i,k} | \lambda, \sigma, \mu\right] = E\left[E\left[\sum_{k=1}^{\sum_{l=0}^{Y_i} S_{i,l}} Z_{n,i,k} | \sum_{l=0}^{Y_i} S_{i,l}\right] | \lambda, \sigma, \mu\right] \quad (47)$$

$$= E\left[\sum_{l=0}^{Y_i} S_{i,l} | \lambda, \sigma, \mu\right] E[Z_{n,i,1} | \lambda, \sigma, \mu] \quad (48)$$

$$= E[Y_1 | \lambda, \mu] E[S_{1,1} | \sigma] \sum_{i=1}^{n-1} E[Z_{n,i,1} | \mu] \quad (49)$$

- $D_n$ : If  $Y_i, S_{i,l}, Z_{i,j,k}, D_i$  for all  $i, j, l, k$  would be uncorrelated, it would hold

$$E[D_i] = E[D_{i-1}(1 - \prod_{j=0}^{i-1} \prod_{k=0}^{\sum_{l=0}^{Y_j} S_{j,l}} (1 - Z_{i,j,k}))] \quad (50)$$

$$= E[D_{i-1}](1 - E[\prod_{j=0}^{i-1} \prod_{k=0}^{\sum_{l=0}^{Y_j} S_{j,l}} (1 - Z_{i,j,k})]) \quad (51)$$

$$= E[D_{i-1}](1 - E[E[\prod_{j=0}^{i-1} \prod_{k=0}^{\sum_{l=0}^{Y_j} S_{j,l}} (1 - Z_{i,j,k}) | Y, S]]) \quad (52)$$

$$= E[D_{i-1}](1 - E[\prod_{j=0}^{i-1} \prod_{k=0}^{\sum_{l=0}^{Y_j} S_{j,l}} (1 - E[Z_{i,j,k}])]) \quad (53)$$

$$= E[D_{i-1}](1 - E[\prod_{j=0}^{i-1} (1 - E[Z_{i,j,k}])^{\sum_{l=0}^{Y_j} S_{j,l}}]) \quad (54)$$

$$\leq E[D_{i-1}](1 - \prod_{j=0}^{i-1} (1 - E[Z_{i,j,k}])^{E[\sum_{l=0}^{Y_j} S_{j,l}]}) \quad (55)$$

$$= E[D_{i-1}](1 - \prod_{j=0}^{i-1} (1 - E[Z_{i,j,k}])^{E[Y_1]E[S_{1,1}]}) \quad (56)$$

$$E[D_1] = (1 - (1 - E[Z_{1,0,1}])^C) \quad (57)$$

where the third line follows as a compound distribution and the 6'th by Jensens Inequality.  $\square$

**Proposition 6.** *It holds:*

$$V[L_n] = E[\Omega_n]V[D_n Q_n] \quad (58)$$

$$+ E[\Omega_n](1 - E[\Omega_n])E[D_n Q_n]^2 \quad (59)$$

$$V[D_n Q_n] \approx E[D_n]V[Q_n] \quad (60)$$

$$+ E[Q_n]^2 E[D_n](1 - E[D_n]) \quad (61)$$

$$V[Q_n] = E[V[Q_n | \lambda, \sigma, \mu]] \quad (62)$$

$$+ V[E[Q_n | \lambda, \sigma, \mu]] \quad (63)$$

$$V[Q_n | \lambda, \sigma, \mu] = \sum_{i=1}^{n-1} ((V[Y_i | \lambda, \mu] E[S_{i,l} | \sigma]^2 \quad (64)$$

$$+ E[Y_i | \lambda, \mu] V[S_{i,l} | \mu]) E[Z_{n,i,1} | \mu]^2 \quad (65)$$

$$+ E[Y_i | \lambda, \mu] E[S_{i,l} | \sigma] V[Z_{n,i,1} | \mu]) \quad (66)$$

$$V[D_n] \approx E[D_n](1 - E[D_n]) \quad (67)$$

$$V[B_n] \approx CV[Z_{n,i,k}] \quad (68)$$

*Proof.*

- For the variance of  $L_n$  it holds:

$$V[L_n] = E[\Omega_n]^2 V[D_n Q_n] + V[\Omega_n]E[D_n Q_n]^2 + V[\Omega_n]V[D_n Q_n] \quad (69)$$

$$= E[\Omega_n]^2 V[D_n Q_n] + E[\Omega_n](1 - E[\Omega_n])E[D_n Q_n]^2 + E[\Omega_n](1 - E[\Omega_n])V[D_n Q_n] \quad (70)$$

$$= E[\Omega_n]V[D_n Q_n] + E[\Omega_n](1 - E[\Omega_n])E[D_n Q_n]^2 \quad (71)$$

$$V[D_n Q_n] = E[D_n]^2 V[Q_n] + E[Q_n]^2 E[D_n](1 - E[D_n]) + E[D_n](1 - E[D_n])V[Q_n] \quad (72)$$

$$= E[D_n]V[Q_n] + E[Q_n]^2 E[D_n](1 - E[D_n]) \quad (73)$$

- For the variance of  $Q_n$  it holds:

$$V[Q_n] = E[V[Q_n | \lambda, \sigma, \mu]] + V[E[Q_n | \lambda, \sigma, \mu]] \quad (74)$$

and

$$V[Q_n | \lambda, \sigma, \mu] = \sum_{i=1}^{n-1} (V[\sum_{l=0}^{Y_i} S_{i,l}] E[Z_{n,i,1}]^2 + E[\sum_{l=0}^{Y_i} S_{i,l}] V[Z_{n,i,1}]) \quad (75)$$

$$= \sum_{i=1}^{n-1} ((V[Y_i] E[S_{i,l}]^2 + E[Y_i] V[S_{i,l}]) E[Z_{n,i,1}]^2 + E[Y_i] E[S_{i,l}] V[Z_{n,i,1}]) \quad (76)$$

- For  $D_n$ , the inequality

$$V[D_n] \leq E[D_n](1 - E[D_n]) \quad (77)$$

follows directly from the Bhatia Davis inequality

$$Var \leq (Exp - min)(max - Exp) \quad (78)$$

□

**Proposition 7.** When  $Y_i \sim Pois(\Lambda M)$ ,  $\Lambda \sim Gamma(a, b)$ ,  $S_{i,l} \sim Pois(\Sigma)$ ,  $\Sigma \sim Gamma(\alpha, \beta)$ ,  $Z_{n,i,j} \sim Bernoulli(e^{(i-n)M})$  (Bernoulli over complementary CDF of an exponential distribution),  $M \sim Gamma(\mathfrak{a}, \mathfrak{b})$  and  $\Omega_i \sim Bernoulli(e^{(i-n)\Delta M})$  it holds:

$$E[Q_n] = \frac{a\alpha + \beta}{b} \mathfrak{a} \mathfrak{b}^{\mathfrak{a}} ((n-i) + \mathfrak{b})^{-\mathfrak{a}-1} \quad (79)$$

$$E[D_i] \approx E[D_{i-1}] \left(1 - \Pi_{j=0}^{i-1} \left(1 - \left(1 + \frac{i-j}{\mathfrak{b}}\right)^{-(\mathfrak{a})}\right)^{\frac{\mathfrak{a}\mathfrak{a}}{\mathfrak{b}\mathfrak{b}} \frac{\alpha}{\beta}}\right) \quad (80)$$

$$E[B_n] = C \left(1 + \frac{n-i}{\mathfrak{b}}\right)^{-(\mathfrak{a})} \quad (81)$$

$$E[\Omega_n] = \left(1 + \frac{n}{\Delta \mathfrak{b}}\right)^{-(\mathfrak{a})} \quad (82)$$

and

$$V[Q_n] = \sum_{i=1}^{n-1} \left[ \left( \frac{a}{b^2} + \frac{a^2}{b} \right) \left( \frac{\alpha}{\beta^2} + \frac{\alpha + \beta^2}{\beta} \right) \right. \quad (83)$$

$$\left. \mathfrak{a} \mathfrak{b}^{\mathfrak{a}} ((2n-2i) + \mathfrak{b})^{-\mathfrak{a}-1} \right] \quad (84)$$

$$+ \frac{a}{b} \left( \frac{\alpha}{\beta^2} + \frac{\alpha + \beta^2}{\beta} \right) \quad (85)$$

$$(\mathfrak{b}^{\mathfrak{a}} \mathfrak{a}(\mathfrak{a}+1)(2n+2i+\mathfrak{b})^{-\mathfrak{a}-2} \quad (86)$$

$$+ \mathfrak{a} \mathfrak{b}^{\mathfrak{a}} ((2n-2i) + \mathfrak{b})^{-\mathfrak{a}-1}) \quad (87)$$

$$+ \frac{a}{b} \frac{\alpha}{\beta} \mathfrak{a} \mathfrak{b}^{\mathfrak{a}} ((2n-2i) + \mathfrak{b})^{-\mathfrak{a}-1} \quad (88)$$

$$+ \frac{a}{b} \frac{\alpha + \beta}{\beta} \mathfrak{a} \mathfrak{b}^{\mathfrak{a}} \quad (89)$$

$$((n-i+\mathfrak{b})^{-\mathfrak{a}-1} - (2n-2i+\mathfrak{b})^{-\mathfrak{a}-1}) \quad (90)$$

$$+ \frac{a^2 \alpha + \beta^2}{b} \sum_{1 \leq i \leq j < n} \quad (91)$$

$$[\mathfrak{b}^{\mathfrak{a}} \mathfrak{a}(\mathfrak{a}+1)(2n-i-j+\mathfrak{b})^{-\mathfrak{a}-2} \quad (92)$$

$$- \mathfrak{a}^2 \mathfrak{b}^{2\mathfrak{a}} ((n-i+\mathfrak{b})(n-j+\mathfrak{b})^{-\mathfrak{a}-1}] \quad (93)$$

$$+ \left( \frac{a^2}{b} \frac{\alpha}{\beta^2} + \frac{a}{b^2} \frac{\alpha + \beta^2}{\beta} + \frac{a}{b^2} \frac{\alpha}{\beta^2} \right) \quad (94)$$

$$\left( \left[ \sum_{i=1}^{n-1} \mathfrak{a} \mathfrak{b}^{\mathfrak{a}} (n-i+\mathfrak{b})^{-\mathfrak{a}-1} \right]^2 \right) \quad (95)$$

$$+ \sum_{1 \leq i \leq j < n} [\mathfrak{b}^{\mathfrak{a}} \mathfrak{a}(\mathfrak{a}+1)(2n-i-j+\mathfrak{b})^{-\mathfrak{a}-2} \quad (96)$$

$$- \mathfrak{a}^2 \mathfrak{b}^{2\mathfrak{a}} ((n-i+\mathfrak{b})(n-j+\mathfrak{b})^{-\mathfrak{a}-1}]) \quad (97)$$

$$V[B_n] = C \left(1 + \frac{n-i}{\mathfrak{b}}\right)^{-(\mathfrak{a})} - \left(1 + \frac{n-i}{\mathfrak{b}}\right)^{-2(\mathfrak{a})} \quad (98)$$

$$V[\Omega_n] = \left(1 + \frac{n}{\Delta \mathfrak{b}}\right)^{-(\mathfrak{a})} - \left(1 + \frac{n}{\Delta \mathfrak{b}}\right)^{-(2\mathfrak{a})} \quad (99)$$

*Proof.* • For  $Q_n$  it holds

$$E\left[\sum_{k=1}^{\sum_{l=0}^Y S_{i,l}} Z_{n,i,k} | \lambda, \sigma, \mu\right] = E[Y_1 | \lambda, \mu] E[S_{1,1} | \sigma] E[Z_{n,i,1} | \mu] \quad (100)$$

$$= \lambda \mu (\sigma + 1) e^{(i-n)\mu} \quad (101)$$

$$E[\lambda] = \frac{a}{b} \quad (102)$$

$$V[\lambda] = \frac{a}{b^2} \quad (103)$$

$$E[\sigma + 1] = \frac{\alpha + \beta}{\beta} \quad (104)$$

$$V[\sigma + 1] = \frac{\alpha}{\beta^2} \quad (105)$$

$$E[\mu e^{(i-n)\mu}] = \int_0^\infty \mu e^{(i-n)\mu} \frac{\mathfrak{b}^\mathfrak{a} \mu^{\mathfrak{a}-1} e^{-\mathfrak{b}\mu}}{\Gamma(\mathfrak{1})} d\mu \quad (106)$$

$$= \mathfrak{a} \mathfrak{b}^\mathfrak{a} (n - i + \mathfrak{b})^{-\mathfrak{a}-1} \quad (107)$$

and thus

$$E[Q_n] = \sum_{i=1}^n \frac{a}{b} \frac{\alpha + \beta}{\beta} \mathfrak{a} \mathfrak{b}^\mathfrak{a} (n - i + \mathfrak{b})^{-\mathfrak{a}-1} \quad (108)$$

Further

$$V[Y_1 | \lambda, \mu] = \lambda^2 \mu + \lambda \mu^2 + \lambda \mu \quad (109)$$

$$V[S_{1,1}\sigma] = \sigma \quad (110)$$

$$E[Z_{n,i,1} | \mu]^2 = e^{((i-n)\mu)^2} \quad (111)$$

$$= e^{(2i-2n)\mu} \quad (112)$$

$$= E[Z_{2n,2i,1}] \quad (113)$$

$$V[Z_{n,i,1} | \mu] = E[Z_{n,i,1} | \mu] - E[Z_{n,i,1} | \mu]^2 \quad (114)$$

$$= E[Z_{n,i,1} | \mu] - E[Z_{2n,2i,1} | \mu] \quad (115)$$

$$= \mathfrak{a} \mathfrak{b}^\mathfrak{a} ((n - i + \mathfrak{b})^{-\mathfrak{a}-1} - (2n - 2i + \mathfrak{b})^{-\mathfrak{a}-1}) \quad (116)$$

We will also need

$$E[\lambda^2] = V[\lambda] + E[\lambda]^2 \quad (117)$$

$$= \frac{a}{b^2} + \frac{a^2}{b} \quad (118)$$

$$E[(\sigma + 1)^2] = V[\sigma + 1] + E[\sigma + 1]^2 \quad (119)$$

$$= \frac{\alpha}{\beta^2} + \frac{\alpha + \beta^2}{\beta} \quad (120)$$

$$E[\mu^2 e^{(2i-2n)\mu}] = \int_0^\infty \mu^2 e^{(2i-2n)\mu} \frac{\mathfrak{b}^\mathfrak{a} \mu^{\mathfrak{a}-1} e^{-\mathfrak{b}\mu}}{\Gamma(\mathfrak{1})} d\mu \quad (121)$$

$$= \frac{\mathfrak{b}^\mathfrak{a} \Gamma(\mathfrak{a} + 2) (2n - 2i + \mathfrak{b})^{-\mathfrak{a}-2}}{\Gamma(\mathfrak{a})} \quad (122)$$

$$= \mathfrak{b}^\mathfrak{a} (\mathfrak{a} + 1) \mathfrak{a} (2n - 2i + \mathfrak{b})^{-\mathfrak{a}-2} \quad (123)$$

Now we know that:

$$E[(V[Y_i|\lambda, \mu]E[S_{i,l}|\sigma]^2E[Z_{n,i,1}|\mu]^2] = E[(\lambda^2\mu + \lambda\mu^2 + \lambda\mu)(\sigma + 1)^2e^{(2i-2n)\mu}] \quad (124)$$

$$= E[\lambda^2]E[(\sigma + 1)^2]E[\mu e^{(2i-2n)\mu}] \quad (125)$$

$$+ E[\lambda]E[(\sigma + 1)^2]E[\mu^2 e^{(2i-2n)\mu}] \quad (126)$$

$$+ E[\lambda]E[(\sigma + 1)^2]E[\mu e^{(2i-2n)\mu}] \quad (127)$$

$$= \left(\frac{a}{b^2} + \frac{a^2}{b}\right)\left(\frac{\alpha}{\beta^2} + \frac{\alpha + \beta^2}{\beta}\right)\mathfrak{a}\mathfrak{b}^{\mathfrak{a}}((2n - 2i) + \mathfrak{b})^{-\mathfrak{a}-1} \quad (128)$$

$$+ \frac{a}{b}\left(\frac{\alpha}{\beta^2} + \frac{\alpha + \beta^2}{\beta}\right)\mathfrak{b}^{\mathfrak{a}}(\mathfrak{a} + 1)\mathfrak{a}(2n + 2i + \mathfrak{b})^{-\mathfrak{a}-2} \quad (129)$$

$$+ \frac{a}{b}\left(\frac{\alpha}{\beta^2} + \frac{\alpha + \beta^2}{\beta}\right)\mathfrak{a}\mathfrak{b}^{\mathfrak{a}}((2n - 2i) + \mathfrak{b})^{-\mathfrak{a}-1} \quad (130)$$

$$E[E[Y_i|\lambda, \mu]V[S_{i,l}|\mu])E[Z_{n,i,1}|\mu]^2] = E[\lambda\mu\sigma e^{(2i-2n)\mu}] \quad (131)$$

$$= E[\lambda]E[\sigma]E[\mu e^{(2i-2n)\mu}] \quad (132)$$

$$= \frac{a}{b}\frac{\alpha}{\beta}\mathfrak{a}\mathfrak{b}^{\mathfrak{a}}((2n - 2i) + \mathfrak{b})^{-\mathfrak{a}-1} \quad (133)$$

and

$$E[E[Y_i|\lambda, \mu]E[S_{i,l}|\sigma]V[Z_{n,i,1}|\mu]] = E[\lambda\mu(\sigma + 1)E[Z_{n,i,1}|\mu] - E[Z_{2n,2i,1}|\mu]] \quad (134)$$

$$= E[\lambda]E[\sigma + 1](E[\mu e^{(i-n)\mu}] - E[\mu e^{(2i-2n)\mu}]) \quad (135)$$

$$= \frac{a}{b}\frac{\alpha + \beta}{\beta}\mathfrak{a}\mathfrak{b}^{\mathfrak{a}}((n - i + \mathfrak{b})^{-\mathfrak{a}-1} - (2n - 2i + \mathfrak{b})^{-\mathfrak{a}-1}) \quad (136)$$

Finally for the second part of the variance we need:

$$V\left[\sum_{i=1}^n \mu e^{(i-n)\mu}\right] = \sum_{1 \leq i \leq j \leq n} \text{Cov}[\mu e^{(i-n)\mu}, \mu e^{(j-n)\mu}] \quad (137)$$

$$= \sum_{1 \leq i \leq j \leq n} E[\mu e^{(i-n)\mu} \mu e^{(j-n)\mu}] - E[\mu e^{(i-n)\mu}]E[\mu e^{(j-n)\mu}] \quad (138)$$

$$= \sum_{1 \leq i \leq j \leq n} E[\mu^2 e^{(i+j-2n)\mu}] - E[\mu e^{(i-n)\mu}]E[\mu e^{(j-n)\mu}] \quad (139)$$

$$= \sum_{1 \leq i \leq j \leq n} \frac{\mathfrak{b}^{\mathfrak{a}} \Gamma(\mathfrak{a} + 2)(2n - i - j + \mathfrak{b})^{-\mathfrak{a}-2}}{\Gamma(\mathfrak{a})} \quad (140)$$

$$- \mathfrak{a}^2 \mathfrak{b}^{\mathfrak{a}} ((n - i + \mathfrak{b})(n - j + \mathfrak{b}))^{-\mathfrak{a}-1} \quad (141)$$

$$V[\lambda(\sigma + 1)] = E[\lambda]^2 V[\sigma + 1] + V[\lambda]E[\sigma + 1]^2 + V[\lambda]V[\sigma + 1] \quad (142)$$

$$= \frac{a^2}{b}\frac{\alpha}{\beta^2} + \frac{a}{b^2}\frac{\alpha + \beta^2}{\beta} + \frac{a}{b^2}\frac{\alpha}{\beta^2} \quad (143)$$

With this we get

$$V[E[Q_n|\lambda, \sigma, \mu]] = V\left[\sum_{i=1}^n E\left[\sum_{k=1}^{\sum_{l=0}^Y S_{i,l}} Z_{n,i,k}|\lambda, \sigma, \mu\right]\right] \quad (144)$$

$$= V\left[\sum_{i=1}^n \lambda\mu(\sigma+1)e^{(i-n)\mu}\right] \quad (145)$$

$$= V\left[\lambda(\sigma+1)\sum_{i=1}^n \mu e^{(i-n)\mu}\right] \quad (146)$$

$$= E[\lambda(\sigma+1)]^2 V\left[\sum_{i=1}^n \mu e^{(i-n)\mu}\right] \quad (147)$$

$$+ V[\lambda(\sigma+1)] E\left[\sum_{i=1}^n \mu e^{(i-n)\mu}\right]^2 \quad (148)$$

$$+ V[\lambda(\sigma+1)] V\left[\sum_{i=1}^n \mu e^{(i-n)\mu}\right] \quad (149)$$

$$= \frac{a^2 \alpha + \beta^2}{b} \sum_{1 \leq i \leq j \leq n} (\mathfrak{b}^{\mathfrak{a}}(\mathfrak{a}+1)\mathfrak{a}(2n-i-j+\mathfrak{b})^{-\mathfrak{a}-2} \quad (150)$$

$$- \mathfrak{a}^2 \mathfrak{b}^{2\mathfrak{a}}((n-i+\mathfrak{b})(n-j+\mathfrak{b}))^{-\mathfrak{a}-1}) \quad (151)$$

$$+ \left(\frac{a^2 \alpha}{b} \frac{\alpha}{\beta^2} + \frac{a}{b^2} \frac{\alpha + \beta^2}{\beta} + \frac{a}{b^2} \frac{\alpha}{\beta^2}\right) \left(\sum_{i=1}^n \mathfrak{a} \mathfrak{b}^{\mathfrak{a}}(n-i+\mathfrak{b})^{-\mathfrak{a}-1}\right)^2 \quad (152)$$

$$+ \left(\frac{a^2 \alpha}{b} \frac{\alpha}{\beta^2} + \frac{a}{b^2} \frac{\alpha + \beta^2}{\beta} + \frac{a}{b^2} \frac{\alpha}{\beta^2}\right) \sum_{1 \leq i \leq j \leq n} (\mathfrak{b}^{\mathfrak{a}}(\mathfrak{a}+1)\mathfrak{a}(2n-i-j+\mathfrak{b})^{-\mathfrak{a}-2} \quad (153)$$

$$- \mathfrak{a}^2 \mathfrak{b}^{2\mathfrak{a}}((n-i+\mathfrak{b})(n-j+\mathfrak{b}))^{-\mathfrak{a}-1}) \quad (154)$$

Inserting into propositions 1 and 2 now yields the result.

- For  $D_i$  note the following: As an exponential distribution whose rate is drawn from a Gamma distribution with shape  $\mathfrak{a}$  and rate  $\mathfrak{b}$  is equal to a Lomax Distribution with scale  $\mathfrak{b}$  and shape  $\mathfrak{a}$ , a single  $Z_{i,j,k}$  is equal to a Bernoulli trial over the complementary CDF of the Lomax distribution.

$$E[Z_{i,j,k}] = (1 + \frac{i-j}{\mathfrak{b}})^{-(\mathfrak{a})} \quad (155)$$

$$(156)$$

It therefore holds

$$E[D_i] = E[D_{i-1}] \left(1 - \Pi_{j=0}^{i-1} \left(1 - \left(1 + \frac{i-j}{\mathfrak{b}}\right)^{-(\mathfrak{a})}\right)^{\frac{a}{b} \frac{a}{b} \frac{\alpha}{\beta}}\right) \quad (157)$$

$$E[D_1] = \left(1 - \left(1 - \left(1 + \frac{1}{\mathfrak{b}}\right)^{-(\mathfrak{a})}\right)^C\right) \quad (158)$$

- $B_n$  and  $\Omega_n$  follow by the same argument (Bernoulli trial over the complementary CDF of the Lomax distribution) and insertion into propositions 1 and 2.

□